frontiers | Frontiers in Water

TYPE Original Research
PUBLISHED 17 July 2023
DOI 10.3389/frwa.2023.1220544

OPEN ACCESS

EDITED BY
Soumendra Nath Bhanja,
Oak Ridge National Laboratory (DOE), United States

REVIEWED BY
Shaoda Liu,
Beijing Normal University, China
Fan Wang,
Sun Yat-sen University, China

*CORRESPONDENCE
Ricky Mwangada Mwanake
✉ ricky.mwanake2@kit.edu

RECEIVED 10 May 2023
ACCEPTED 26 June 2023
PUBLISHED 17 July 2023

CITATION
Mwanake RM, Gettel GM, Wangari EG, Butterbach-Bahl K and Kiese R (2023) Interactive effects of catchment mean water residence time and agricultural area on water physico-chemical variables and GHG saturations in headwater streams. *Front. Water* 5:1220544. doi: 10.3389/frwa.2023.1220544

Interactive effects of catchment mean water residence time and agricultural area on water physico-chemical variables and GHG saturations in headwater streams

Ricky Mwangada Mwanake[1]*, Gretchen Maria Gettel[1,2,3], Elizabeth Gachibu Wangari[1], Klaus Butterbach-Bahl[1,4] and Ralf Kiese[1]

[1]Karlsruhe Institute of Technology, Institute for Meteorology and Climate Research, Atmospheric Environmental Research (IMK-IFU), Garmisch-Partenkirchen, Germany, [2]IHE-Delft Institute for Water Education, Delft, Netherlands, [3]Department of Ecoscience, Lake Ecology, University of Aarhus, Aarhus, Denmark, [4]Pioneer Center Land-CRAFT, Department of Agroecology, University of Aarhus, Aarhus, Denmark

Greenhouse gas emissions from headwater streams are linked to multiple sources influenced by terrestrial land use and hydrology, yet partitioning these sources at catchment scales remains highly unexplored. To address this gap, we sampled year-long stable water isotopes ($\delta^{18}O$ and $\delta^{2}H$) from 17 headwater streams differing in catchment agricultural areas. We calculated mean residence times (MRT) and young water fractions (YWF) based on the seasonality of $\delta^{18}O$ signals and linked these hydrological measures to catchment characteristics, mean annual water physico-chemical variables, and GHG % saturations. The MRT and the YWF ranged from 0.25 to 4.77 years and 3 to 53%, respectively. The MRT of stream water was significantly negatively correlated with stream slope ($r^2 = 0.58$) but showed no relationship with the catchment area. Streams in agriculture-dominated catchments were annual hotspots of GHG oversaturation, which we attributed to precipitation-driven terrestrial inputs of dissolved GHGs for streams with shorter MRTs and nutrients and GHG inflows from groundwater for streams with longer MRTs. Based on our findings, future research should also consider water mean residence time estimates as indicators of integrated hydrological processes linking discharge and land use effects on annual GHG dynamics in headwater streams.

KEYWORDS

water-stable isotopes, mean residence time, young-water-fraction, carbon dioxide, methane, nitrous oxide, water-chemistry, land use

Introduction

Headwater streams are recognized as important hotspots for riverine greenhouse gas (CO_2, CH_4, and N_2O) emissions, contributing significantly to global warming (Raymond et al., 2013; Yao et al., 2020; Rosentreter et al., 2021). The disproportionately large contribution from these ecosystems relative to large streams is due to their large surface–area-to-volume ratio, which allows close connectivity to GHG sources, such as the

hyporheic zone and the surrounding landscape (Hotchkiss et al., 2015; Turner et al., 2015; Marzadri et al., 2017). Apart from instream biogeochemical production, GHG concentrations in these ecosystems may also originate from external sources, such as groundwater or terrestrial land uses via interflow originating from near-saturated soil water (e.g., Borges et al., 2015; Hotchkiss et al., 2015). These external sources are most important when hydrological connectivity among the streams, soil water, and groundwater is activated, particularly during high precipitation events. However, source partitioning of these GHGs among soil water, groundwater, and *in situ* production at catchment scales, which will be crucial in designing localized mitigation strategies, remains largely unexplored (Marx et al., 2017; Duvert et al., 2018). The reason is that separating *in situ* from *ex situ* GHG sources is highly challenging, and the ratios can vary widely across temporal (i.e., discharge conditions) and spatial scales (i.e., catchment land use) (e.g., Aho and Raymond, 2019; Borges et al., 2019; Mwanake et al., 2019, 2022).

Stable water isotopes ($\delta^{18}O$ and $\delta^{2}H$) can be used as conservative water tracers to identify the contributions of different water sources to stream discharge and define integrated hydrological processes at catchment scales (Kendall and Caldwell, 1998). The conservative nature of water isotopic tracers is advantageous compared to gaseous tracers, such as CFCs and He. While the latter two can be used to estimate travel times for groundwater effectively, they are unsuited for surface waters as they are not conserved during their transit, making them inappropriate for evaluating whole-catchment hydrological processes (Kirchner, 2016). Mixing models using source-specific stable water isotope signatures have been previously used to partition the dominating runoff sources within catchments (e.g., Soulsby et al., 2000; McGuire et al., 2002). Alternatively, stream water's mean residence time (MRT) and young water fraction (YWF) within a catchment can also be used as simple measures to characterize the dominant water sources of stream discharge formation (DeWalle et al., 1997; Wolock et al., 1997; Kirchner, 2016). Stream water (or catchment) MRT describes the effects of storage and mixing within the catchment in terms of its temporal response to precipitation inputs (Dunn et al., 2007), while the YWF represents the water fraction of stream flow <2 months in age (Kirchner, 2016). Both parameters can help describe essential hydrological conditions controlling solute retention and transport downstream (e.g., Farrick and Branfireun, 2015), as well as production and consumption processes, e.g., of biogeochemical nutrient cycling (McGuire and McDonnell, 2006; Kirchner, 2016).

Seasonality in $\delta^{18}O$ isotopic composition of stream and precipitation water has been used to estimate MRT and YWF with sine-wave-based lumped parameter models (e.g., Soulsby et al., 1999; Rodgers et al., 2005; Kirchner, 2016). Catchments with stream water dominated by fast precipitation interflow through terrestrial soils have shorter MRTs and higher YWFs. In contrast, groundwater-dominated streams are characterized by longer MRTs and lower YWFs (Kirchner, 2016). Based on the relationships between MRTs and quantified instream solutes and GHG concentrations, inferring their origins to the above sources may be possible. Yet, despite the potential benefits of using the stable isotopes of either H_2O or C and N as tracers to constrain solute and GHG sources in fluvial ecosystems, such studies are still scarce (Jurado et al., 2018; e.g., Campeau et al., 2018; Horgby et al., 2019), and none of the existing studies have specifically used stable water isotopes.

Within lotic ecosystems, agricultural land use has been shown to increase riverine GHG concentrations by either supporting internal production through the supply of nutrients and labile carbon or as a direct external source of dissolved GHGs (e.g., Drake et al., 2019; Mwanake et al., 2022, 2023). Apart from describing water storage and transit processes within a catchment, the MRTs and YWFs of stream water could also help to explain better how catchments respond to anthropogenic nutrient and dissolved GHG inputs from agricultural areas (e.g., Ensign and Doyle, 2006) and their subsequent cycling that results in the *in situ* formation of riverine GHGs.

Therefore, this study aimed to determine the potential of using the MRTs and YWFs of headwater catchments within Germany differing in upstream agricultural land use areas to infer the primary instream solute and GHG sources. Specifically, we aimed (1) to determine the seasonal variation in water stable isotopes across catchments differing in geomorphic and climatic conditions, (2) to estimate the MRT and the YWF in the catchments and identify their relationships with catchment size, slope, and elevation, and (3) to determine the effect of agricultural land use on mean annual dissolved oxygen (DO), dissolved inorganic nitrogen (DIN), dissolved organic carbon (DOC), and greenhouse gas (CO_2, CH_4, N_2O) % saturations across streams with different MRTs and YWFs.

Materials and methods

Study area

Five headwater catchments in the southwest (Neckar/Goldersbach, Neckar/Ammer, Neckar/Steinlach), central (Schwingbach), and southeast (Loisach), Germany, were selected for this study. The catchments covered various sizes and were dominated mainly by mixed forests and agricultural (i.e., cropland and fertilized grasslands) ecosystems (Table 1; Figure 1). The Goldersbach is primarily a forested catchment (95%), while the Steinlach catchment is dominated by forests (74%), with agricultural lands (croplands and grasslands) and settlement areas occupying 21% and 5% of the landscape, respectively. In contrast to the Goldersbach and Steinlach, the Ammer catchment (outlet Pfäffingen) is dominated by croplands (80%), with 11% forests and 9% settlement areas (Figure 1C). The climatology of the three catchments is warm and temperate (Cfb, Köppen climate classification), with a mean annual rainfall of 923 mm (monthly mean min: 63 mm, monthly mean max: 98 mm) (1999 – 2019) and a mean annual temperature of 9.3°C (monthly mean min: 0.2°C, monthly mean max: 18.6°C) (1991–2021) (Climate-data.org, Link).

The Schwingbach catchment is of mixed land use, with 41% forest, 46% croplands, 8% settlement areas, and 5% pasturelands (Wangari et al., 2022) (Figure 1A). The climatology of the region is warm and temperate (Cfb, Köppen climate classification), with an annual rainfall of 742 mm (monthly mean

TABLE 1 Characteristics of the 17 stream sites in the Loisach, Neckar, and Schwingbach catchments.

Catchment	Site code	Catchment area (Ha)	Slope (m m^{-1})	Elevation (m)	MAT (°C)	MAP (mm)	Agricultural area %	Main Land use
Loisach	FL1	40	0.4	750	3.8	1,693	14	Forest
Loisach	FL2	75	0.02	756	3.8	1,693	1	Forest
Loisach	FL3	102	0.15	719	3.8	1,693	0	Forest
Loisach	GL1	11	0.06	660	3.8	1,693	100	Agricultural
Loisach	GL2	13	0.045	663	3.8	1,693	81	Agricultural
Neckar/ Ammer	CN1	26157	0.067	379	9.3	923	89	Agricultural
Neckar/ Goldersbach	FN1	11623	0.077	366	9.3	923	3	Forest
Neckar/ Steinlach	FN2	51332	0.044	348	9.3	923	26	Forest
Schwingbach	CS1	5345	0.026	189	9.8	742	56	Agricultural
Schwingbach	CS2	60	0.042	187	9.8	742	100	Agricultural
Schwingbach	CS3	220	0.011	260	9.8	742	53	Agricultural
Schwingbach	CS4	2337	0.026	183	9.8	742	63	Agricultural
Schwingbach	FS1	268	0.014	204	9.8	742	17	Forest
Schwingbach	FS2	67	0.044	334	9.8	742	14	Forest
Schwingbach	FS3	41	0.018	297	9.8	742	4	Forest
Schwingbach	FS4	220	0.081	272	9.8	742	35	Forest
Schwingbach	FS5	62	0.018	241	9.8	742	2	Forest

min: 51 mm, monthly mean max: 72 mm) (1999–2019) and a mean annual temperature of 9.8°C (monthly mean min: 1.3°C, monthly mean max: 18.8°C) (1991–2021) (Climate-data.org, Link). The Upper Loisach catchment (outlet Eschenlohe town) is located within the German alpine region. The catchment has steep slopes and valley bottoms. The catchment's land use comprises forests interspersed with natural grasslands and rocky surfaces on the mountain slopes (78%). At the valley bottom, the land use is mainly settlement areas (9%), fertilized grasslands (8%), and wetlands (5%) (Figure 1B). The climatology is cold and temperate (Dfb, Köppen climate classification), with annual precipitation of 1,693 mm (monthly mean min: 87 mm, monthly mean max: 207 mm) (1999–2019) and mean annual temperature of 3.8°C (monthly mean min: −6.6°C, monthly mean max: 13.1°C) (1991–2021) (Climate-data.org, Link).

Sampling strategy

Within the five headwater catchments, 17 streams were sampled for water stable isotope analysis every 2–3 weeks covering a whole year (Table 1, Figure 1). The Schwingbach and Loisach catchments were sampled from June 2020 to June 2021, while the Goldersbach, Ammer, and Steinlach catchments were sampled from April 2021 to April 2022. The sites were distributed across catchments with differing percentages of agricultural land area (See Mwanake et al., 2023 for details) (Table 1).

Water sampling and stable isotope measurements

Water samples from the 17 sites were filtered onsite through 0.45 μm filters and collected in acid-washed 30 ml HDPE bottles for transportation to the laboratory. In the laboratory, the samples were stored frozen for later analysis of stable water isotopes ($\delta^{18}O$ and $\delta^{2}H$) by cavity ring-down spectroscopy with an L2140-i isotopic water analyzer (precision: ±0.025 $\delta^{18}O$ and ± 0.1‰ $\delta^{2}H$) (Picarro, Inc., Santa Clara, USA). The isotope values were reported as per mill (‰) relative to the Vienna Standard Mean Ocean Water (VSMOW). D_excess values were calculated from $\delta^{18}O$ and $\delta^{2}H$ isotopic signals in stream water (Equation 1). The aim was to use the values to determine the impact of evaporation, precipitation, and storage on the isotopic signatures of stream water (Reckerth et al., 2017).

$$d_{excess} = \delta^{2}H - 8\delta^{18}O \quad (1)$$

Because we lacked yearlong consistent water stable isotope samples from precipitation across the five catchments, we retrieved that data from long-term sampling (1978–2013) of

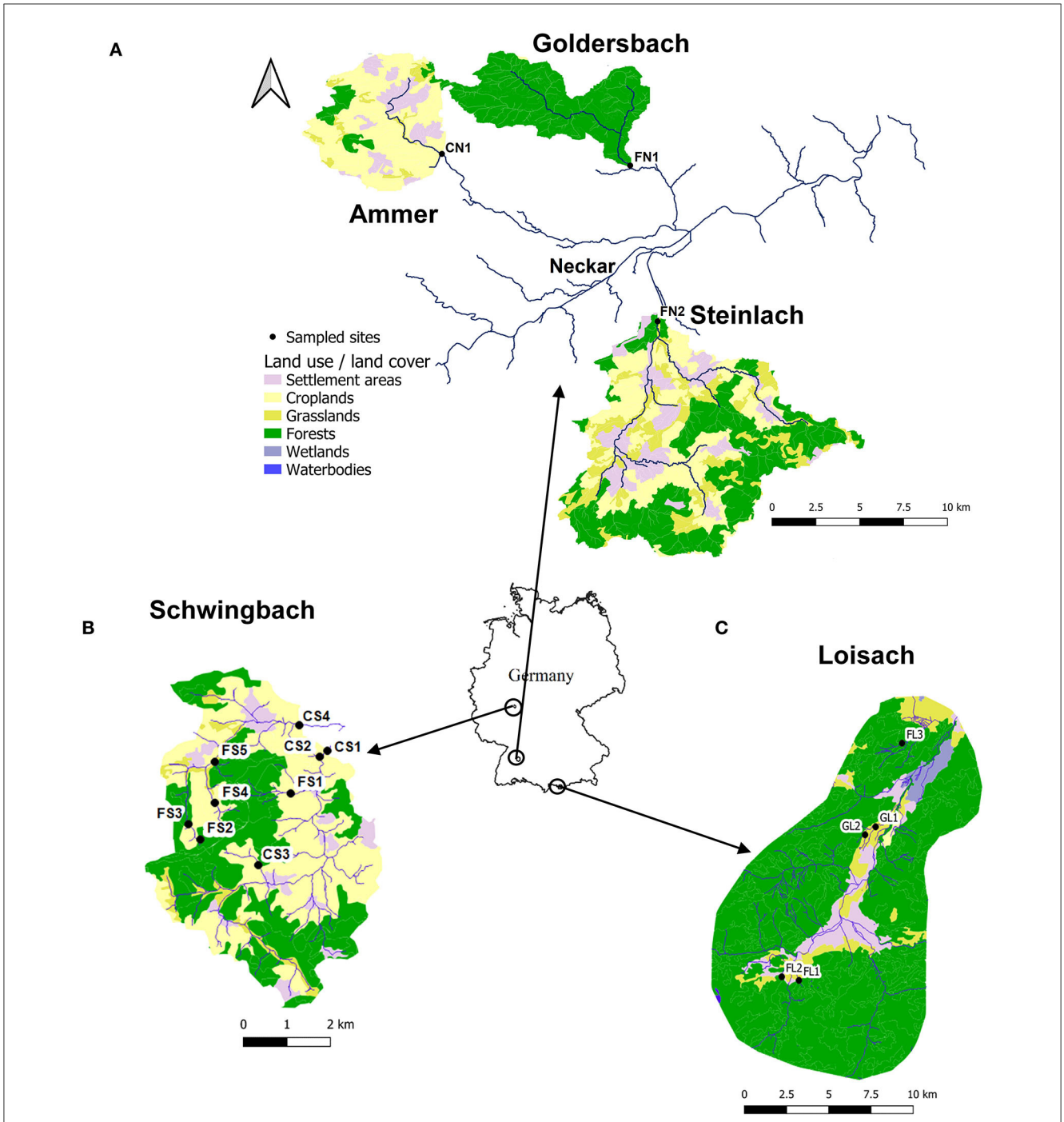

FIGURE 1
Land cover maps of the **(A)** Neckar catchments (Goldersbach, Ammer, and Steinlach), **(B)** Schwingbach, and **(C)** Loisach derived from the Corine Land Cover 2018 inventory with a 25-ha spatial resolution (https://land.copernicus.eu/pan-european/corine-land-cover/clc2018?tab=mapview). Black dots with labels represent the 17 sampled streams and rivers.

precipitation from a German network of climate stations.[1] Climate stations for this study were chosen based on the proximity to our sites and elevation similarities, thus Garmisch-Partenkirchen (730 a.s.l) for the Loisach, Koblenz (100 a.s.l) for the Schwingbach, and Stuttgart (330 a.s.l) for the Neckar catchment sites.

Annual datasets for water physico-chemical variables and GHG saturations

Based on 2- to 3-week measuring intervals, annual means of water physico-chemical variables and GHG saturations were calculated from previously published work, where stable water isotope sampling in this study was conducted in tandem (see detailed methods in Mwanake et al., 2023). In brief, water

1 https://nucleus.iaea.org/wiser/index.aspx

temperature (°C) and dissolved oxygen (DO) (saturation %) were measured using the Pro DSS multiprobe (YSI Inc., USA). DIN concentrations were determined using colorimetric methods on a microplate spectrophotometer (Model: Epoch, BioTek Inc., USA). The DOC and TDN concentrations were measured using a TOC/TN analyzer (Analytica-Jena; multi N/C 3100, Germany).

GHG samples in water were collected in triplicates simultaneously with the water physico-chemical samples using the headspace equilibration technique (Raymond et al., 1997; Mwanake et al., 2022). GHG concentrations from the headspace were analyzed using an SRI gas chromatograph (8610C, Germany) with an electron capture detector (ECD) for N_2O and a flame ionization detector (FID) with an upstream methanizer for simultaneous measurements of CH_4 and CO_2 concentrations. Dissolved GHG concentrations in the stream water were calculated from post-equilibration gas concentrations in the headspace after correcting for atmospheric (ambient) GHG concentrations and then expressed as percentages of the atmospheric concentrations (GHG saturation).

Estimating MRT and YWF from seasonal trends of δ^{18}o in stream and precipitation water

Previous hydrological studies have used three main model types to represent a residence time distribution function that describes how the $\delta^{18}O$ isotopic composition of stream water at a given outflow point is a function of past lagged inputs from precipitation water (McGuire and McDonnell, 2006). These include the dispersion model (DM), the exponential model (EM), and the exponential-piston model (EPM). In this study, we described the residence time distribution function based on the much simpler EM model using the sine-wave approach to estimate the MRT in which precipitation inputs are assumed to mix rapidly with resident water in the soil and groundwater storage zones (Małoszewski et al., 1983; McDonnell et al., 1991).

To determine the MRT of each of our 17 streams (using the "sinreg" function in the "ShellChron" package in R), we first fitted sine wave curves to the temporal trends of $\delta^{18}O$ values in stream and precipitation water of the entire year (Equation 2) (DeWalle et al., 1997). The goodness of fit was assessed based on the coefficient of determination (r^2) and the hypothesis significance testing *p*-value. In the equation, $\delta^{18}O$ refers to the simulated annual $\delta^{18}O$, I refers to the yearly average of the measured $\delta^{18}O$ value, A refers to the seasonal amplitude of the measured $\delta^{18}O$ value in precipitation or stream water, b refers to the duration of the yearly cycle in days, t is time in days, and C refers to the phase lag or time at which $\delta^{18}O$ peaks in radians.

$$\delta^{18}O = I + A\sin[\frac{2\pi t}{b} + C] \quad (2)$$

The MRT was then calculated using Equation 3, where As is the seasonal amplitude of $\delta^{18}O$ in stream water, Ap is the seasonal amplitude of $\delta^{18}O$ for precipitation, and b' is the radial frequency constant (0.017294 rad d^{-1}). The young water fraction (YWF) at each site was approximated as the ratio between stream and precipitation water amplitudes from the sinusoidal regressions expressed as a percent (Kirchner, 2016).

$$MRT = \frac{1}{b'}[(As/Ap)^{-2} - 1]^{0.5} \quad (3)$$

Statistical analysis

We estimated the stream and local meteoric water lines (LMWL; long-term precipitation) based on the site-specific linear regression analysis of $\delta^{18}O$ and $\delta^{2}H$ isotopic signals. Linear regression analysis was also used to investigate the relationships of estimated MRT and YWF with the catchment characteristics slope, catchment area, and elevation ("lm" function in R). The 2D contour plots based on interpolations using means ("interp2xyz" function in R) were used to determine the interactive effects of catchment MRTs and agricultural areas on annual means of physico-chemical variables and GHG concentrations in streams.

Results

Spatial–temporal variability in stable water isotopes

The magnitude and temporal trends of stable water isotopes in streams varied among the three main catchments, following general differences in elevation and seasonal temperature and precipitation variation (Table 1 and Supplementary Table S1). In the Loisach catchment, which is more elevated and has colder annual temperatures than the other two catchments, $\delta^{18}O$ (‰, VSMOW) values in streams ranged from −12.02‰ to −8.81‰ (mean ± SD; −10.78 ± 0.6 ‰) (Figure 2, Supplementary Table S1). However, more enriched stream water isotopic signals were quantified in the Neckar (−10.72‰ to −8.25‰, −9.15 ± 0.37‰) and Schwingbach (−8.92‰ to −7.71‰, −8.36 ± 0.25‰) catchments (Figure 2). Similar trends were also found for the $\delta^{2}H$ values, which were more enriched along elevation gradients in the order of the Loisach (−93.73‰ to −65.64‰, −82.41 ± 5.5‰), Neckar (-83.41‰ to −61.15‰, −69.06 ±3.1‰), and Schwingbach (−65.85‰ to −58.12‰, −62.32 ± 1.5‰) catchments (Figure 2 and Table 1). The relationship between hydrogen and oxygen isotopes of stream water in the Loisach catchment had a slope of 8.64, which was close to that of the local meteoric water line (LMWL) of long-term precipitation in Garmisch (8.12) (Figure 2). In contrast, the slope of this relationship was much lower in the Neckar and Schwingbach catchments (7.42 and 5.66, respectively), with the latter catchment deviating from the LMWL of long-term precipitation by as much as 30% (Figure 2).

The $\delta^{18}O$ and $\delta^{2}H$ stream water isotopic signals in the Neckar and Schwingbach catchments were also more seasonally dampened than in the Loisach catchment, with occasional declines in spring and peaks in summer at some streams in the Neckar catchment (Figure 3). The stable water isotopes in the streams of the Loisach were more enriched in summer and autumn similar to precipitation patterns (Supplementary Figure S1), and

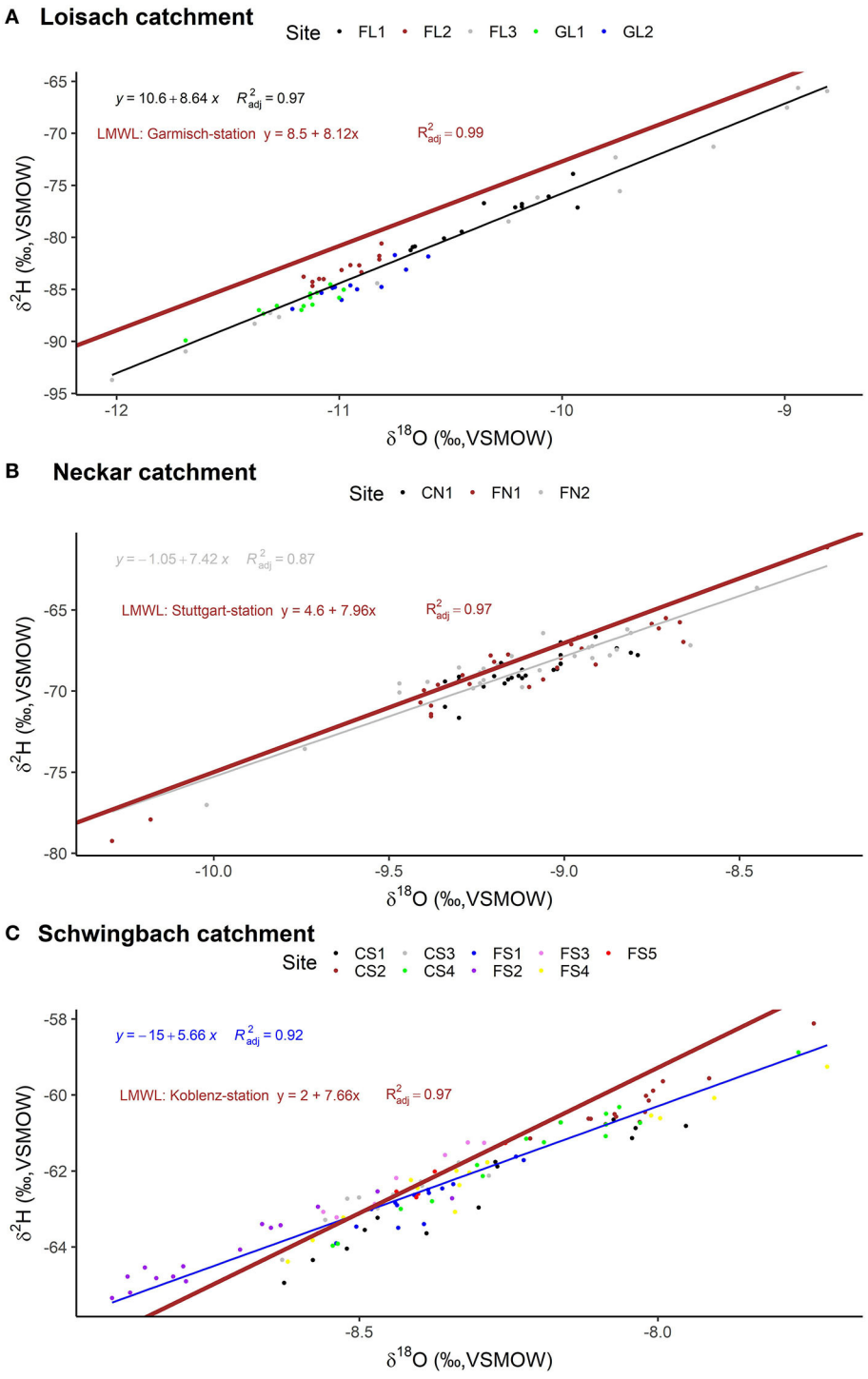

FIGURE 2
Comparisons of $\delta^{18}O$ and $\delta^{2}H$ linear relationships of stream water across the three catchments with the respective LMWL of precipitation water (In brown) from the **(A)** Garmisch, **(B)** Stuttgart, and **(C)** Koblenz stations (Supplementary Figure S1, Supplementary Table S1). The graphs' text represents the relationships' slopes, intercepts, and r^2.

then declined at the transition into the winter season (Figure 3). The sites within the catchment with highest annual $\delta^{18}O$ and $\delta^{2}H$ variabilities were the FL1 and FL3 sites, which had peak values during the summer period comparable to precipitation trends (Figure 3, Supplementary Figure S1). Like the stable water isotopes, d_excess signals in streams also had distinct temporal trends. They ranged from 1.69‰ to 6.07‰ (3.81 ± 1.07‰) in the Loisach, 1.93‰ to 6.22‰ (4.18 ± 0.94‰) in the Neckar, and 2.48‰ to 6.33‰ (4.54 ± 0.74‰) in the Schwingbach (Figure 3). In the Schwingbach and Neckar catchments, peak

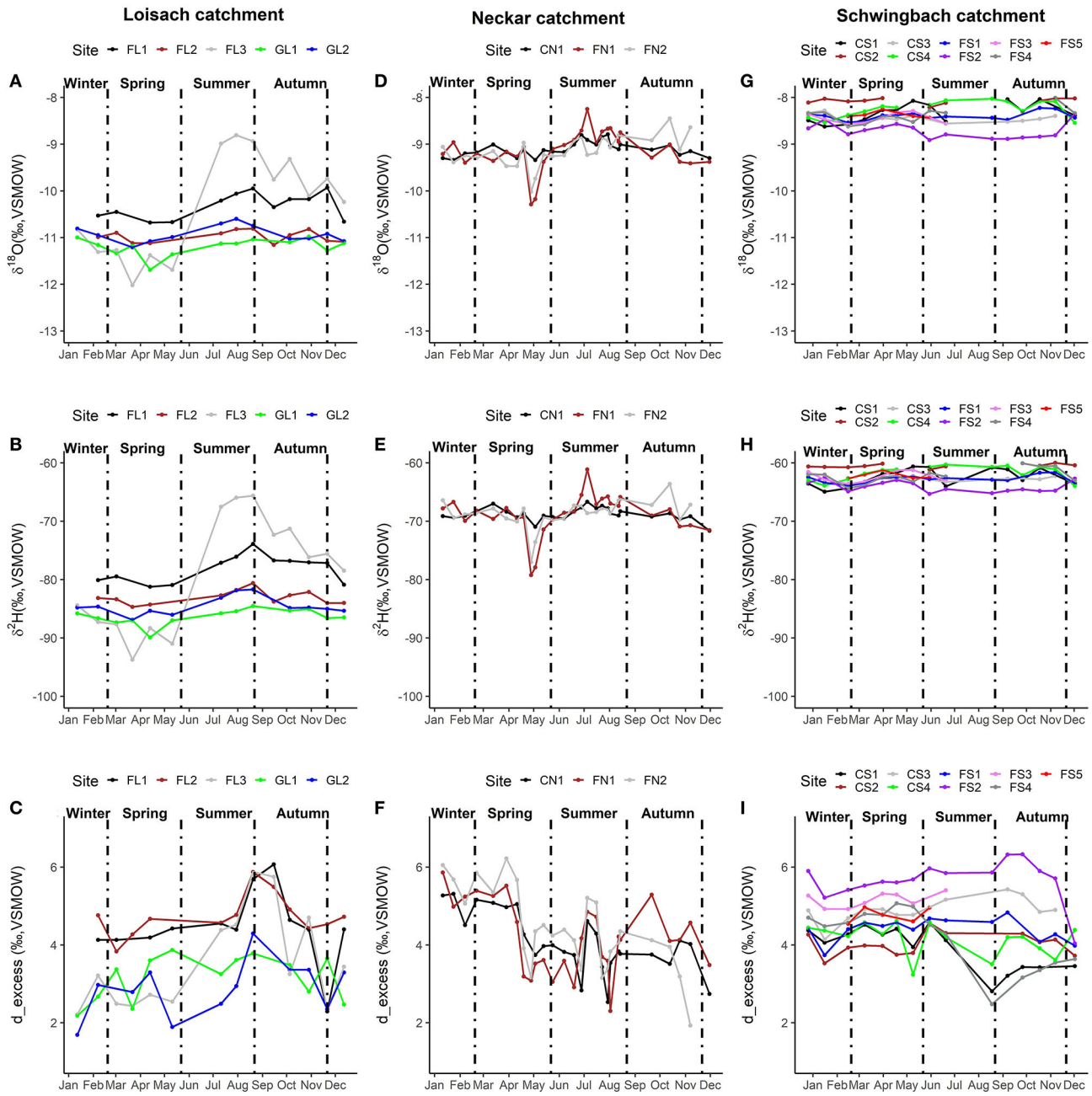

FIGURE 3
Temporal trends of $\delta^{18}O$, $\delta^{2}H$, and d_excess isotopic signals of stream water at the 17 sites within the Loisach **(A–C)**, Neckar **(D–F)**, and Schwingbach **(G–I)** catchments.

d_excess values were recorded in winter and spring but declined in most sites in summer as temperatures increased (Figure 3). However, during the autumn period, d_excess values within the streams of the two catchments increased, following precipitation patterns that also peaked in that period (Figure 3, Supplementary Figure S1). Contrary to the Schwingbach and Neckar catchments, d_excess signals in the Loisach streams mostly mimicked precipitation trends. They increased from winter to the beginning of autumn before declining again in winter (Figure 3, Supplementary Figure S1).

MRTs and YWFs

Sinusoidal regressions significantly ($p < 0.05$) predicted the annual seasonal trends in $\delta^{18}O$ signals of precipitation and stream water, with r^2 values ranging from 0.34 to 0.97 (Table 2, Supplementary Figure S2). Stream water's mean residence times (MRTs) spanned two orders of magnitude, ranging from 93 to 1741 days (0.25–4.77 years). The lowest MRT value was observed at the FL1 site in the Loisach catchment, while the highest MRT value was found at the FL2 site

TABLE 2 Summary statistics outlining the performance of sinusoidal regressions in fitting temporal trends of precipitation and stream water $\delta^{18}O$ isotopic signals.

Catchment	Site/ station	Source	Sinusoidal regression statistics		Annual amplitude	Estimated MRT		
			R^2	*P*-value		YWF (%)	Days	Years
Loisach	Garmisch	Precipitation	0.97	<0.001	3.89			
Loisach	FL1	Stream	0.51	0.016	2.06	53	93	0.25
Loisach	FL2	Stream	0.47	0.024	0.13	3	1741	4.77
Loisach	FL3	Stream	0.93	<0.001	1.42	36	147	0.40
Loisach	GL1	Stream	0.42	0.027	0.48	12	463	1.27
Loisach	GL2	Stream	0.52	0.015	0.83	21	265	0.73
Neckar	Stuttgart	Precipitation	0.97	<0.001	2.47			
Neckar/ Ammer	CN1	Stream	0.49	<0.001	0.17	7	864	2.37
Neckar/ Goldersbach	FN1	Stream	0.41	<0.001	0.38	15	369	1.01
Neckar/ Steinlach	FN2	Stream	0.48	<0.001	0.36	15	392	1.07
Schwingbach	Koblenz	Precipitation	0.93	<0.001	2.28			
Schwingbach	CS1	Stream	0.56	0.004	0.24	11	546	1.49
Schwingbach	CS2	Stream	0.45	0.021	0.13	6	983	2.69
Schwingbach	CS3	Stream	0.34	0.062	0.10	4	1377	3.77
Schwingbach	CS4	Stream	0.57	0.002	0.23	10	584	1.60
Schwingbach	FS1	Stream	0.35	0.037	0.08	4	1641	4.50
Schwingbach	FS2	Stream	0.34	0.032	0.17	8	758	2.08
Schwingbach	FS3	Stream	0.94	<0.001	0.15	7	888	2.43
Schwingbach	FS4	Stream	0.89	<0.001	0.51	22	255	0.70
Schwingbach	FS5	Stream	0.90	0.040	0.09	4	1402	3.84

within the same catchment but with a lower stream slope (Table 1).

Stream water MRTs were significantly negatively related to stream slopes ($r^2 = 0.58$) but had no significant relationships with catchment area or elevation (Figure 4). Like the MRT, the young water fractions (YWFs) of each site, which signals fast responses to precipitation inputs that result in water residence times <2 months, varied widely, ranging from 3% to 53% of stream flow (Table 2). The YWFs were positively correlated with stream slope ($r^2 = 0.75$) and elevation ($r^2 = 0.28$) but showed no significant correlation with the catchment area (Figure 4).

Interactive effects of MRT and agricultural area on stream water physico-chemical variables and GHG saturations

Mean annual DO saturation, DIN, TDN, and DOC concentrations at the 17 stream sites ranged from 65 to 111%, 0.6–7.2 mg-N L^{-1}, 0–1.7 mg-N L^{-1}, 0.6–8.9 mg-N L^{-1}, and 1.5–6.1 mg-C L^{-1}, respectively (Supplementary Table S2). Interactions between MRTs and the agricultural areas controlled the spatial trends in water physico-chemical properties. At streams within catchments with low (< 25%) agricultural areas, instream DO saturation was mainly >100%, with little differences across water ages as indicated by the MRTs (Figure 5). In contrast, DO saturation gradually decreased with decreasing MRTs at streams within catchments with high (>75%) agricultural areas (Figure 5). Grassland-dominated streams (GL1 and GL2) in the Loisach mainly drove these trends as they had the lowest DO saturations and lowest MRTs (Figure 5).

Interactions between water ages and agricultural areas also impacted DIN and TDN stream concentrations. Streams within catchments with low agricultural areas had mostly low DIN and TDN concentrations and showed less variability across the water ages. However, at catchments with high agricultural areas, DIN and TDN concentrations in streams gradually increased with MRTs (Figure 5). The highest DIN and TDN concentrations were found at the CN1 site in the Neckar, with 89% cropland area and a MRT of 2.5 years. Contrary to DO and dissolved nitrogen concentrations, DOC concentrations were mainly higher at streams dominated by forested land uses (<50% agricultural areas) across all water ages.

Mean annual GHG % saturations indicated that most of the streams were supersaturated with reference to atmospheric equilibrium concentrations and ranged from 110 to 1157%

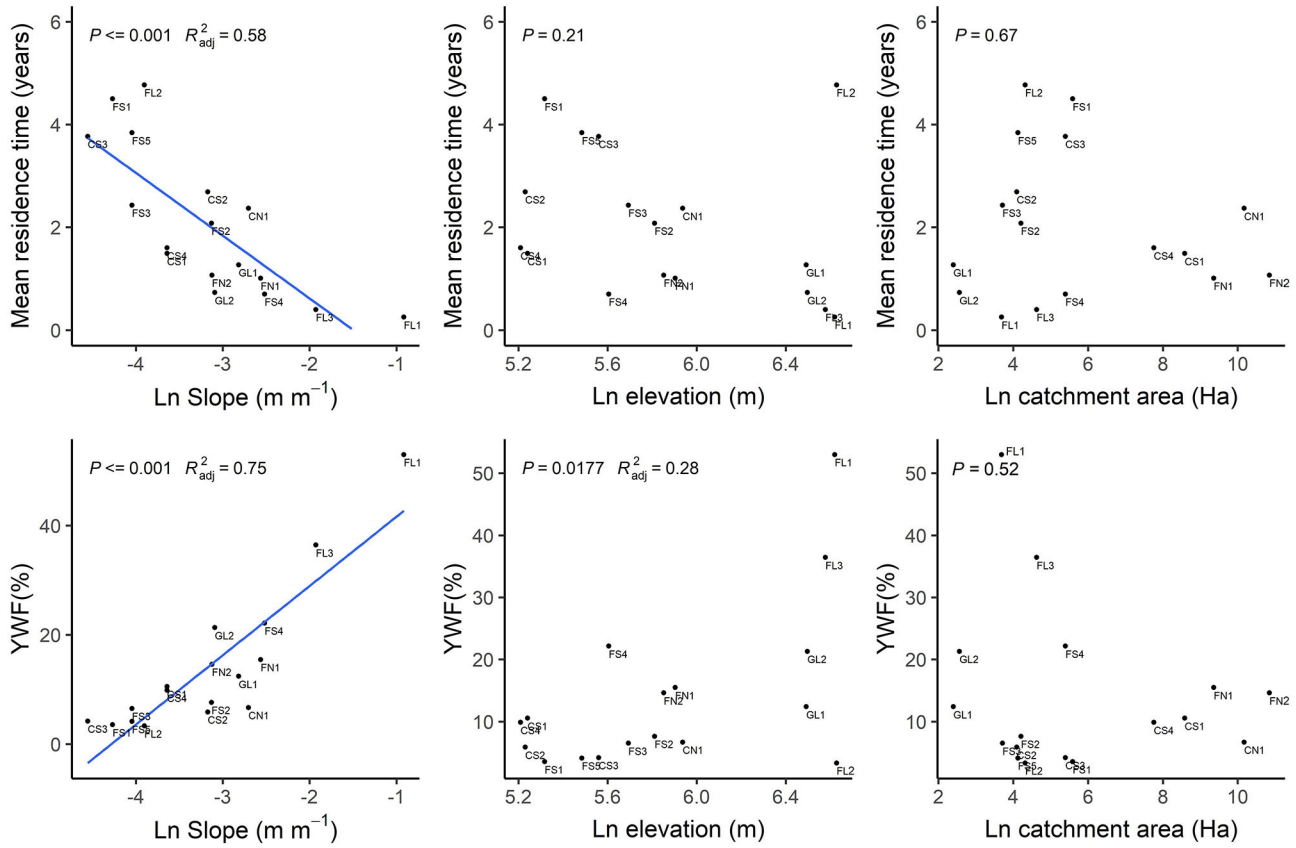

FIGURE 4
Scatter plots indicating the relationships of the mean water residence times and YWF at the 17 catchments (Site labels added) with slope, elevation, and catchment area characteristics. The blue line shows the best fit linear regression, with the text indicating the *p*-value and r^2 of the fit.

for CO_2, 279–10416% for CH_4, and 92–491 for N_2O (Supplementary Table S2). Interactions of MRTs and agricultural land use also affected GHG % saturations. Peak CO_2 % saturations were found at streams with either low agricultural areas and longer MRTs or high agricultural areas and shorter MRTs. The latter trends were driven mainly by the two fertilized grassland sites (GL1 and GL2) in the Loisach catchment, which also had the lowest DO % saturations. Similar patterns as CO_2 were also found for CH_4 % saturations, where the two streams within fertilized grassland with shorter MRTs had the highest CH_4 % saturations. As for N_2O, peak values were mainly at sites with high agricultural areas across all water ages, with the highest N_2O % saturation found at a cropland site (CS4) in the Schwingbach catchment. Like CO_2 % saturation, additional N_2O saturation peaks were found at streams with longer MRTs and low agricultural areas.

Discussion

Spatial–temporal variability in stable water isotopes

The spatial–temporal patterns of $\delta^{18}O$ and $\delta^{2}H$ isotopic signals in streams within the Loisach, Neckar, and Schwingbach catchments followed altitudinal and, thus, temperature gradients, similar to several other studies in temperate ecosystems (Halder et al., 2015; Reckerth et al., 2017). The higher seasonal dampening of $\delta^{18}O$ and $\delta^{2}H$ isotopic signals of stream water in the Neckar and Schwingbach catchments relative to the Loisach catchment suggests that most streams within these catchments are mainly groundwater-fed (Figure 3). Our findings agree with previous studies, which found significant groundwater contributions to stream discharge within the two catchments (Orlowski et al., 2016; Glaser et al., 2020). In contrast to streams in the Neckar and Schwingbach catchments, $\delta^{18}O$ and $\delta^{2}H$ isotopic signals in the Loisach were more seasonally variable, with summer and autumn peaks coinciding with rainfall events. This finding suggests possible fast responses to rain precipitation in these steep-sloping streams characteristic of the Loisach catchment, accounting for the more enriched $\delta^{18}O$ and $\delta^{2}H$ isotopic signals in summer and autumn. Inter-site variabilities were also higher in this catchment, which we contend reflects differing contributions of precipitation and groundwater among the streams within the catchment due to variable slope conditions (Table 1, Figure 3).

Stream water $\delta^{18}O$ and $\delta^{2}H$ linear relationships also mirrored temperature and elevation gradients among the three catchments. Lower slope values of these relationships were found in the Neckar and Schwingbach streams compared to their local meteoric water

10.3389/frwa.2023.1220544

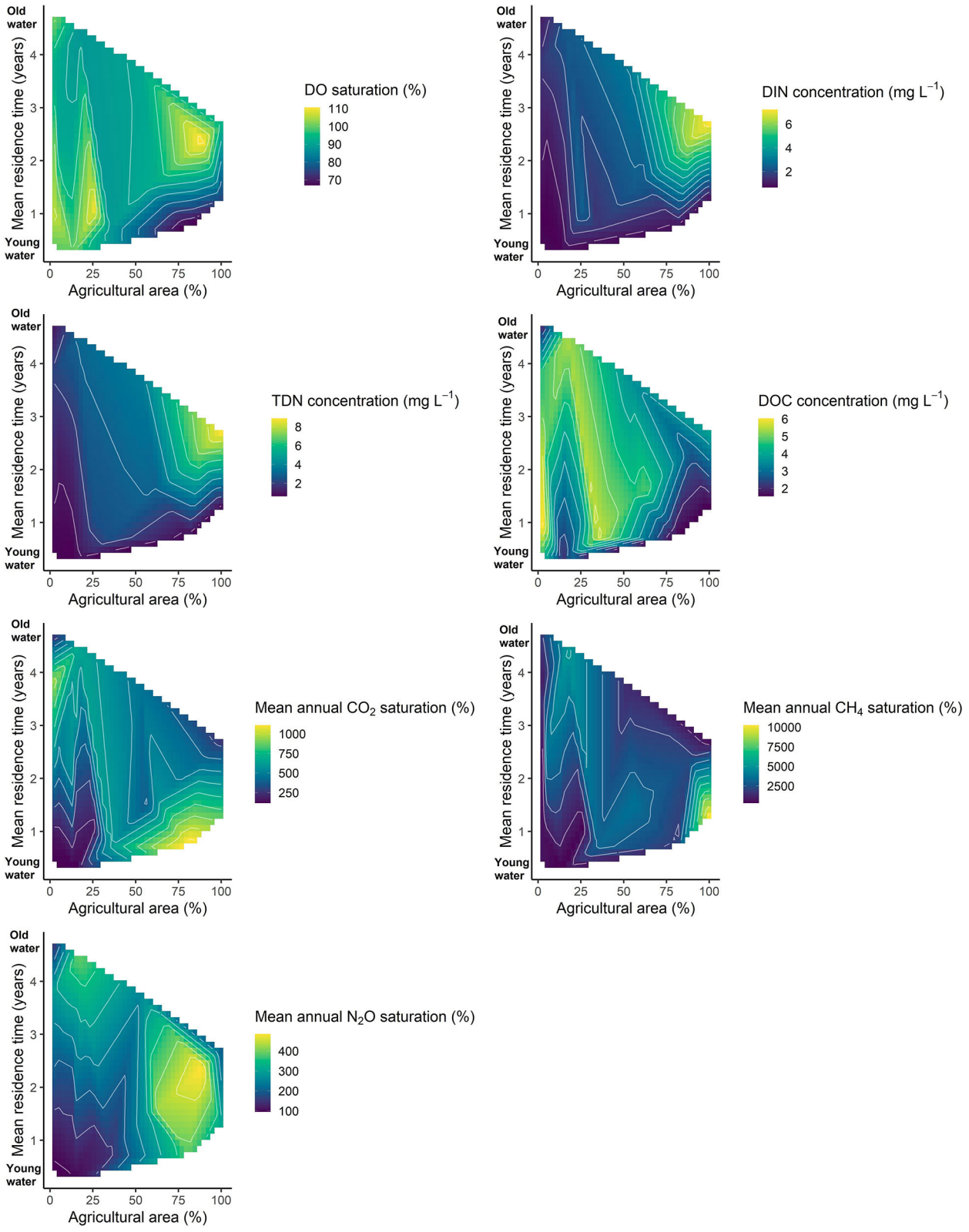

FIGURE 5
2D contour plots indicating the interactive effects of mean water residence times and agricultural areas on mean annual stream water, DIN, TDN, and DOC concentrations and GHG % saturation.

lines (LMWL), indicating higher evaporation effects at higher temperatures and lower altitudes than the Loisach streams. The d_excess values in the two catchments also primarily decreased as the seasons transitioned from winter to warmer spring and summer seasons, indicating fractionation effects due to evaporation on the $\delta^{18}O$ and $\delta^{2}H$ stream water isotopic signals (e.g., Reckerth et al., 2017). Conversely, $\delta^{18}O$ and $\delta^{2}H$ relationships in the Loisach catchment showed impacts of different precipitation forms rather than evaporation. Snowfall within the catchment during winter months resulted in heavily depleted isotopic signals, while rain precipitation during the summer and autumn months accounted for the more enriched isotopic signals and higher d_excess values, accounting for the wide intra-annual variabilities in $\delta^{18}O$, $\delta^{2}H$, and d_excess signals (Figure 3). In contrast to the Reckerth et al. (2017) study dominated by large rivers, the d_excess values in the headwaters of this study occasionally reflected those in rain precipitation, particularly in summer and autumn for the Loisach catchment and in autumn for the Neckar and Schwingbach catchments. This finding suggests that while d_excess values in larger rivers may primarily reflect evaporation effects, those in headwater streams, which are closely connected to the surrounding landscape, may also indicate periods of substantial contributions of rainfall to stream flow.

Drivers of stream water MRTs and YWFs

The ranges of the MRTs of stream water quantified in this study are comparable to several studies of similar catchment sizes, applying sine-wave-based exponential models (Table 2) (0.13–>5 years: McGuire and McDonnell, 2006). Although other studies have found significant relationships between MRT and catchment area (e.g., Wolock et al., 1997; Farrick and Branfireun, 2015; Zhou et al., 2021), we found no such relationships in this study. Instead, we found a significant relationship between MRT and stream slope, whereby the MRT of streams decreased with increasing stream slopes (Figure 4). Catchment slope can significantly impact the MRT of water by controlling how streams respond to precipitation and groundwater inputs (e.g., Rodgers et al., 2005; McGuire et al., 2005). We contend that steeper slopes generally result in faster precipitation interflow through soils, resulting in shorter MRTs. Similar results have also been found for other steep sloping streams (e.g., Asano et al., 2002; Katsuyama et al., 2010). However, gentle sloping catchments typically have slower stream water flow with higher groundwater contributions, resulting in longer MRTs. The strong positive relationship between YWFs and stream slopes further supports this conclusion.

Agricultural effects on mean annual water-physico-chemical variables and GHG saturations along stream water MRT gradients

While GHG dynamics of headwater catchments in this study were previously discussed by Mwanake et al. (2023), the results of this study have contributed to a better conceptualization of catchment-scale land use effects linked to hydrological processes. We found notable differences in mean annual water physico-chemical properties and GHG saturations among streams of catchments differing in agricultural areas and MRTs. Among the water physico-chemical variables, dissolved nitrogen forms (DIN and TDN) had the most unidirectional trends with MRTs and agricultural areas. Catchments with the longest MRTs, lowest YWFs, and highest agricultural areas tended to have the highest dissolved nitrogen (e.g., CN1 and CS4). This finding suggests that longer water transit times through nitrogen-rich agricultural soils resulted in accumulated mineral nitrogen in the sub-surface water, which is eventually transported to groundwater during hydrological connectivity. These findings agree with those from a previous modeling study, which found that most groundwater aquifers in agricultural regions within Germany were contaminated with excess nitrogen (Knoll et al., 2020). In contrast to dissolved nitrogen forms, similar spatial trends with MRTs were not found for DOC, as the highest concentrations were mainly at forested-dominated catchments, findings that indicate the significant role of forests in supplying allochthonous carbon to streams (e.g., Aitkenhead-Peterson et al., 2003). In contrast to the dissolved nitrogen forms, an increase in the agricultural area tended to support higher mean annual dissolved GHG inputs at streams with shorter MRTs and higher YWFs (e.g., GL1 and GL2), suggesting an inflow of dissolved GHGs, possibly from the GHG-rich agricultural soils during precipitation. These trends also reflect findings in terrestrial ecosystems, which have found agricultural soils to be hot spots of GHGs (e.g., Raich and Tufekciogul, 2000; Wangari et al., 2022). The above findings suggest that the annual oversaturation of GHGs within agricultural streams, as found in several other studies (e.g., Borges et al., 2018; Herreid et al., 2021; Mwanake et al., 2022, 2023), could be supported either by younger precipitation interflows through oversaturated soils or older groundwater nutrients.

Conceptually, we contend that the contribution of either process will depend on stream slopes and the magnitude of precipitation-driven discharge events. Previous fluvial studies have found that during peak discharge periods with short water residence times, instream biogeochemical process rates are low (Alexander et al., 2009; Masese et al., 2017) and are, therefore, less correlated with instream GHG fluxes (e.g., Hampton et al., 2020; Mwanake et al., 2022). As such, dissolved GHG inputs from terrestrial soils may contribute to elevated riverine GHGs during those periods. This mechanism may explain our findings in the steep sloping catchments in the Loisach catchment (GL1 and GL2), which were dominated by GHG-rich agricultural soils.

In contrast, contaminated groundwater inputs, which support nutrient intake to streams that may favor *in situ* GHG production, account for high GHG concentrations during base flow conditions. We found both elevated N_2O and TDN concentrations at streams with relatively long MRTs and high agricultural areas, findings that support the above mechanism as N_2O production in streams is generally stimulated by nitrogen inputs (e.g., Borges et al., 2018; Mwanake et al., 2019). Such a mechanism may be especially relevant in gentle-sloping catchments with considerable agricultural influences, such as those found in the Schwingbach

and Neckar catchments (CN1 and CS4). At gentle-sloping forested streams (<25% agricultural areas) with relatively long MRTs, groundwater effects on *in situ* production may have also dominated CO_2 and CH_4 dynamics. We found elevated CO_2, CH_4, and DOC concentrations within these streams, indicating that the latter variable may have fueled respiratory production of the two gaseous carbon losses during baseflow conditions.

Conclusion

This study demonstrates the importance of catchment scale hydrological processes on land-use-related solute and GHG dynamics in catchments of differing slopes. It also provides crucial insights into how precipitation interflows through soils and groundwater, characterized by different MRT, affect instream water physico-chemical properties and GHG saturations. We found that streams in agriculture-dominated catchments show higher GHG oversaturation than forested catchments based on two fundamental mechanisms. These mechanisms are elevated terrestrial interflows of dissolved GHGs during high precipitation-driven discharge periods for steep-sloping streams and nutrient inputs by groundwater during base flow conditions for gentle-sloping streams, which favor *in situ* GHG production.

While this study has demonstrated that estimates of MRT within catchments based on stable water isotopes can be valuable tools in deciphering integrated catchment processes that control solute and GHG dynamics, our values are not without uncertainties. These uncertainties stem from our use of simplified sine wave-based lumped parameter models, which have been occasionally found to underestimate mean residence time estimates (McGuire and McDonnell, 2006). Despite these potential uncertainties in the exact magnitudes of our estimated MRTs, this study represents an initial empirical step in conceptually linking hydrological and biogeochemical processes that govern instream solute and GHG dynamics, which we found to be strongly linked to catchment characteristics of slopes and surrounding land use. We recommend that future studies should focus on higher temporal resolution (events, sub-yearly) analysis of stream water GHG saturation and discharge, in addition to measurements of stable water isotopes in precipitation, groundwater, and soil water, to improve MRT estimates and decouple internal and external sources of fluvial GHG emissions.

Data availability statement

The original contributions presented in the study are included in the article/Supplementary material, further inquiries can be directed to the corresponding authors.

Author contributions

RM, RK, GG, and KB-B designed the field experiments. RK provided the infrastructural funding. RM and EW did the field and laboratory work. RM did the statistical analysis and consulted with RK. RM prepared the first draft manuscript, consulting with RK, KB-B, and GG. All authors contributed to the article and approved the submitted version.

Funding

This research was funded by the German academic exchange service (DAAD) as part of RM's doctoral studies. Infrastructure for the research was provided by the TERENO Bavarian Alps/Pre-Alps Observatory, and funded by the Helmholtz Association and the Federal Ministry of Education and Research (BMBF).

Acknowledgments

The authors thank the entire laboratory staff at Karlsruhe Institute of Technology, Campus Alpin, Justus Liebig University Giessen, and the University of Tübingen for supporting the gas and nutrient analyses. We also acknowledge the contributions of Prof. Dr. Lutz Breuer, Dr. Tobias Houska of the University of Giessen, and Dr. Clarissa Glaser of the University of Tübingen for their logistical support.

Conflict of interest

The authors declare that the research was conducted in the absence of any commercial or financial relationships that could be construed as a potential conflict of interest.

Publisher's note

Supplementary material

The Supplementary Material for this article can be found online at: https://www.frontiersin.org/articles/10.3389/frwa.2023.1220544/full#supplementary-material

References

Aho, K. S., and Raymond, P. A. (2019). Differential response of greenhouse gas evasion to storms in forested and wetland streams. *J. Geophys. Res. Biogeosci.* 124, 649–662. doi: 10.1029/2018JG004750

Aitkenhead-Peterson, J. A., McDowell, W. H., and Neff, J. C. (2003). *Sources, Production, and Regulation of Allochthonous Dissolved Organic Matter Inputs to Surface Waters. Aquatic Ecosystems* (London: Academic Press), 25–70.

Alexander, R. B., Böhlke, J. K., Boyer, E. W., David, M. B., Harvey, J. W., Mulholland, P. J., et al. (2009). Dynamic modeling of nitrogen losses in river networks unravels the coupled effects of hydrological and biogeochemical processes. *Biogeochemistry* 93, 91–116. doi: 10.1007/s10533-008-9274-8

Asano, Y., Uchida, T., and Ohte, N. (2002). Residence times and flow paths of water in steep unchannelled catchments, Tanakami, Japan. *J. Hydrol.* 261, 173–192. doi: 10.1016/S0022-1694(02)00005-7

Borges, A. V., Darchambeau, F., Lambert, T., Bouillon, S., Morana, C., Brouyère, S., et al. (2018). Effects of agricultural land use on fluvial carbon dioxide, methane and nitrous oxide concentrations in a large European river, the Meuse (Belgium). *Sci. Total Environ.* 611, 342–355. doi: 10.1016/j.scitotenv.2017.08.047

Borges, A. V., Darchambeau, F., Lambert, T., Morana, C., Allen, G. H., Tambwe, E., et al. (2019). Variations in dissolved greenhouse gases (CO_2,CH_4, N_2O) in the Congo river network overwhelmingly driven by fluvial-wetland connectivity. *Biogeosciences* 16, 3801–3834. doi: 10.5194/bg-16-3801-2019

Borges, A. V., Darchambeau, F., Teodoru, C. R., Marwick, T. R., Tamooh, F., Geeraert, N. (2015). Globally significant greenhouse gas emissions from African inland waters. *Nature Geoscience* 8, 637–642. doi: 10.1038/ngeo2486

Campeau, A., Bishop, K., Nilsson, M. B., Klemedtsson, L., Laudon, H., Leith, F. I., et al. (2018). Stable carbon isotopes reveal soil-stream DIC linkages in contrasting headwater catchments. *J. Geophysical Res. Biogeosciences* 123, 149–167. doi: 10.1002/2017JG004083.

DeWalle, D. R., Edwards, P. J., Swistock, B. R., Aravena, R., and Drimmie, R. J. (1997). Seasonal isotope hydrology of three Appalachian forest catchments. *Hydrolo. Processes* 11, 1895–1906. doi: 10.1002/(SICI)1099-1085(199712)11:15andlt;1895::AID-HYP538andgt;3.0.CO;2-#

Drake, T. W., Van Oost, K., Barthel, M., Bauters, M., Hoyt, A. M., Podgorski, D. C., et al. (2019). Mobilization of aged and biolabile soil carbon by tropical deforestation. *Nat. Geosci.* 12, 541–546. doi: 10.1038/s41561-019-0384-9

Dunn, S. M., McDonnell, J. J., and Vach,é, K. B. (2007). Factors influencing the residence time of catchment waters: a virtual experiment approach. *Water Res. Res.* 43, 393. doi: 10.1029/2006WR005393

Duvert, C., Butman, D. E., Marx, A., Ribolzi, O., and Hutley, L. B. (2018). CO_2 evasion along streams driven by groundwater inputs and geomorphic controls. *Nat. Geosci.* 11, 813–818. doi: 10.1038/s41561-018-0245-y

Ensign, S. H., and Doyle, M. W. (2006). Nutrient spiraling in streams and river networks. *J. Geophys. Res. Biogeosci.* 111, 114. doi: 10.1029/2005JG000114

Farrick, K. K., and Branfireun, B. A. (2015). Flowpaths, source water contributions and water residence times in a Mexican tropical dry forest catchment. *J. Hydrol.* 529, 854–865. doi: 10.1016/j.jhydrol.2015.08.059

Glaser, C., Schwientek, M., Junginger, T., Gilfedder, B. S., Frei, S., Werneburg, M., et al. (2020). Comparison of environmental tracers including organic micropollutants as groundwater exfiltration indicators into a small river of a karstic catchment. *Hydrol. Proc.* 34, 4712–4726. doi: 10.1002/hyp.13909

Halder, J., Terzer, S., Wassenaar, L. I., Araguás-Araguás, L. J., and Aggarwal, P. K. (2015). The Global Network of Isotopes in Rivers (GNIR): integration of water isotopes in watershed observation and riverine research. *Hydrol. Earth Syst. Sci.* 19, 3419–3431. doi: 10.5194/hess-19-3419-2015

Hampton, T. B., Zarnetske, J. P., and Briggs, M. A., MahmoodPoor Dehkordy, F., Singha, K., Day-Lewis, F. D., and Lane, J. W. (2020). Experimental shifts of hydrologic residence time in a sandy urban stream sediment–water interface alter nitrate removal and nitrous oxide fluxes. *Biogeochemistry* 149, 195–219. doi: 10.1007/s10533-020-00674-7

Herreid, A. M., Wymore, A. S., Varner, R. K., Potter, J. D., and McDowell, W. H. (2021). Divergent controls on stream greenhouse gas concentrations across a land-use gradient. *Ecosystems* 24, 1299–1316. doi: 10.1007/s10021-020-00584-7

Horgby, Å., Boix Canadell, M., Ulseth, A. J., Vennemann, T. W., and Battin, T. J. (2019). High-resolution spatial sampling identifies groundwater as driver of CO_2 dynamics in an Alpine stream network. *J. Geophys. Res. Biogeosci.* 124, 1961–1976. doi: 10.1029/2019JG005047

Hotchkiss, E. R., Hall Jr, R. O., Sponseller, R. A., Butman, D., Klaminder, J., Laudon, H., et al. (2015). Sources of and processes controlling CO_2 emissions change with the size of streams and rivers. *Nat. Geosci.* 8, 696–699. doi: 10.1038/ngeo2507

Jurado, A., Borges, A., Pujades, E., Briers, P., Nikolenko, O., Dassargues, A., et al. (2018). Dynamics of greenhouse gases in the river–groundwater interface in a gaining river stretch (Triffoy catchment, Belgium). *Hydrogeol. J.* 2, 1–14. doi: 10.1007/s10040-018-1834-y

Katsuyama, M., Tani, M., and Nishimoto, S. (2010). Connection between streamwater mean residence time and bedrock groundwater recharge/discharge dynamics in weathered granite catchments. *Hydrol. Proc.* 24, 2287–2299. doi: 10.1002/hyp.7741

Kendall, C., and Caldwell, E. A. (1998). Fundamentals of Isotope Geochemistry. Isotope Tracers in Catchment Hydrology. (New York, NY: Elsevier), 51–86.

Kirchner, J. W. (2016). Aggregation in environmental systems–Part 1: Seasonal tracer cycles quantify young water fractions, but not mean transit times, in spatially heterogeneous catchments. *Hydrol. Earth Syst. Sci.* 20, 279–297. doi: 10.5194/hess-20-279-2016

Knoll, L., Breuer, L., and Bach, M. (2020). Nation-wide estimation of groundwater redox conditions and nitrate concentrations through machine learning. *Environ. Res. Lett.* 15, 064004. doi: 10.1088/1748-9326/ab7d5c

Małoszewski, P., Rauert, W., Stichler, W., and Herrmann, A. (1983). Application of flow models in an alpine catchment area using tritium and deuterium data. *J. Hydrol.* 66, 319–330. doi: 10.1016/0022-1694(83)90193-2

Marx, A., Dusek, J., Jankovec, J., Sanda, M., Vogel, T., van Geldern, R., et al. (2017). A review of CO_2 and associated carbon dynamics in headwater streams: a global perspective. *Rev. Geophys.* 55, 560–585. doi: 10.1002/2016RG000547

Marzadri, A., Dee, M. M., Tonina, D., Bellin, A., and Tank, J. L. (2017). Role of surface and subsurface processes in scaling N_2O emissions along riverine networks. *Proc. Nat. Acad. Sci.* 114, 4330–4335. doi: 10.1073/pnas.1617454114

Masese, F. O., Salcedo-Borda, J. S., Gettel, G. M., Irvine, K., and McClain, M. E. (2017). Influence of catchment land use and seasonality on dissolved organic matter composition and ecosystem metabolism in headwater streams of a Kenyan river. *Biogeochemistry* 132, 1–22. doi: 10.1007/s10533-016-0269-6

McDonnell, J. J., Stewart, M. K., and Owens, I. F. (1991). Effect of catchment-scale subsurface mixing on stream isotopic response. *Water Res. Res.* 27, 3065–3073. doi: 10.1029/91WR02025

McGuire, K. J., DeWalle, D. R., and Gburek, W. J. (2002). Evaluation of mean residence time in subsurface waters using oxygen-18 fluctuations during drought conditions in the mid-Appalachians. *J. Hydrol.* 261, 132–149. doi: 10.1016/S0022-1694(02)00006-9

McGuire, K. J., and McDonnell, J. J. (2006). A review and evaluation of catchment transit time modeling. *J. Hydrol.* 330, 543–563. doi: 10.1016/j.jhydrol.2006.04.020

McGuire, K. J., McDonnell, J. J., Weiler, M., Kendall, C., McGlynn, B. L., Welker, J. M., et al. (2005). The role of topography on catchment-scale water residence time. *Water Res. Res.* 41, 657. doi: 10.1029/2004WR003657

Mwanake, R. M., Gettel, G. M., Aho, K. S., Namwaya, D. W., Masese, F. O., Butterbach-Bahl, K., and Raymond, P. A. (2019). Land use, not stream order, controls N_2O concentration and flux in the upper Mara River basin, Kenya. *J. Geophys Res Biogeosci.* 124, 3491–3506. doi: 10.1029/2019JG005063

Mwanake, R. M., Gettel, G. M., Ishimwe, C., Wangari, E. G., Butterbach-Bahl, K., and Kiese, R. (2022). Basin-scale estimates of greenhouse gas emissions from the Mara River, Kenya: Importance of discharge, stream size, and land use/land cover. *Limnol. Oceanograph.* 67, 1776–1793. doi: 10.1002/lno.12166

Mwanake, R. M., Gettel, G. M., Wangari, E. G., Glaser, C., Houska, T., Breuer, L., et al. (2023). Anthropogenic activities significantly increase annual greenhouse gas (GHG) fluxes from temperate headwater streams. *EGUsphere*. 2023, 1–46. doi: 10.5194/egusphere-2023-683

Orlowski, N., Kraft, P., Pferdmenges, J., and Breuer, L. (2016). Exploring water cycle dynamics by sampling multiple stable water isotope pools in a developed landscape in Germany. *Hydrol. Earth Syst. Sci.* 20, 3873–3894. doi: 10.5194/hess-20-3873-2016

Raich, J. W., and Tufekciogul, A. (2000). Vegetation and soil respiration: correlations and controls. *Biogeochemistry* 48, 71–90. doi: 10.1023/A:1006112000616

Raymond, P. A., Caraco, N. F., and Cole, J. J. (1997). Carbon dioxide concentration and atmospheric flux in the Hudson river. *Estuaries* 20, 381–390. doi: 10.2307/1352351

Raymond, P. A., Hartmann, J., Lauerwald, R., Sobek, S., McDonald, C., Hoover, M., et al. (2013). Global carbon dioxide emissions from inland waters. *Nature* 503, 355–359. doi: 10.1038/nature12760

Reckerth, A., Stichler, W., Schmidt, A., and Stumpp, C. (2017). Long-term data set analysis of stable isotopic composition in German rivers. *J. Hydrol.* 552, 718–731. doi: 10.1016/j.jhydrol.2017.07.022

Rodgers, P., Soulsby, C., Waldron, S., and Tetzlaff, D. (2005). Using stable isotope tracers to assess hydrological flow paths, residence times and landscape influences in a nested mesoscale catchment. *Hydrol. Earth Syst. Sci.* 9, 139–155. doi: 10.5194/hess-9-139-2005

Rosentreter, J. A., Borges, A. V., Deemer, B. R., Holgerson, M. A., Liu, S., Song, C. (2021). Half of global methane emissions come from highly variable aquatic ecosystem sources. *Nat. Geoscience* 14, 225–230. doi: 10.1038/s41561-021-00715-2

Soulsby, C., Malcolm, R., Helliwell, R., and Ferrier, R. C. (1999). Hydrogeochemsitry of montane springs and their influence on streams in the Cairngorm mountains, Scotland. *Hydrol. Earth Syst. Sci.* 3, 409–419. doi: 10.5194/hess-3-409-1999

Soulsby, C., Malcolm, R., Helliwell, R., Ferrier, R. C., and Jenkins, A. (2000). Isotope hydrology of the Allt a'Mharcaidh catchment, Cairngorms, Scotland: implications for hydrological pathways and residence times. *Hydrol. Proc.* 14, 747–762. doi: 10.1002/(SICI)1099-1085(200003)14:4andlt;747::AID-HYP970andgt;3.0.CO;2-0

Turner, P. A., Griffis, T. J., Lee, X., Baker, J. M., Venterea, R. T., Wood, J. D., et al. (2015). Indirect nitrous oxide emissions from streams within the US Corn Belt scale with stream order. *Proc. Nat. Acad. Sci.* 112, 9839–9843. doi: 10.1073/pnas.1503598112

Wangari, E. G., Mwanake, R. M., Kraus, D., Werner, C., Gettel, G. M., Kiese, R., et al. (2022). Number of chamber measurement locations for accurate quantification of landscape-scale greenhouse gas fluxes: Importance of land use, seasonality, and greenhouse gas type. *J. Geophys. Res. Biogeosci.* 127, 901. doi: 10.1029/2022JG006901

Wolock, D. M., Fan, J., and Lawrence, G. B. (1997). Effects of basin size on low-flow stream chemistry and subsurface contact time in the Neversink River watershed, New York. *Hydrol. Proc.* 11, 1273–1286. doi: 10.1002/(SICI)1099-1085(199707)11:9andlt;1273::AID-HYP557andgt;3.0.CO;2-S

Yao, Y., Tian, H., Shi, H., Pan, S., Xu, R., Pan, N., et al. (2020). Increased global nitrous oxide emissions from streams and rivers in the Anthropocene. *Nat. Clim. Change* 10, 138–142. doi: 10.1038/s41558-019-0665-8

Zhou, J., Liu, G., Meng, Y., Xia, C., Chen, K., Chen, Y., et al. (2021). Using stable isotopes as tracer to investigate hydrological condition and estimate water residence time in a plain region, Chengdu, China. *Sci. Rep.* 11, 2812. doi: 10.1038/s41598-021-82349-3